

## Analysis of HV bushing internal properties using DFR

### An introduction to DFR

DFR (Dielectric Frequency Response), also known as FDS (Frequency Domain Spectroscopy) is a measurement technique in which capacitance and losses (dissipation factor/tan delta or power factor) are measured over multiple frequencies to assess the insulation condition of test objects, such as power transformers, bushings, and current transformers (CTs). DFR technology is a long-established test procedure in laboratories that, in an innovative effort by Megger, was adapted for field use through the IDAX range of instruments.

In power transformers, bushings, and CTs, issues are often not visible under 'convenient' test conditions, such as at ambient temperature and when using line frequency test sources. Rather, problems are magnified at higher temperatures or closer to the operational limits of the objects. DFR measurements, comprised of many individual tan delta (or power factor) measurements, are primarily a function of insulation system geometry, aging byproducts, moisture, insulation liquid conductivity, frequency, and temperature. Using knowledge about this relationship, assessment can be made in the frequency domain, rather than in the much more challenging temperature domain.

In the calculations, ITC (Individual Temperature Correction) - another important Megger innovation - is used to determine DFR results at a desired reference temperature based upon the DFR test data measured at the test object temperature. The IDAX software incorporates ITC frequency sweeps specifically designed for assessment of power transformers, as well as bushings and instrument transformers.

The IDAX DFR method is now part of international guides and standards, e.g., CIGRE TB 254, CIGRE TB 414, CIGRE TB 445, CIGRE TB 775, IEEE C57.152-2013, and IEEE C57.161-2018.

## DRF response of a normal bushing

In the graph below, a DFR measurement (10 kHz down to 10 mHz) at room temperature (20 °C) of a normal bushing is shown. The uppermost curve is the measured capacitance (right Y-axis) and the lower curve is the dissipation factor divided by 100 to give a percentage, labelled %DF (purple). The lower red curve can be disregarded.

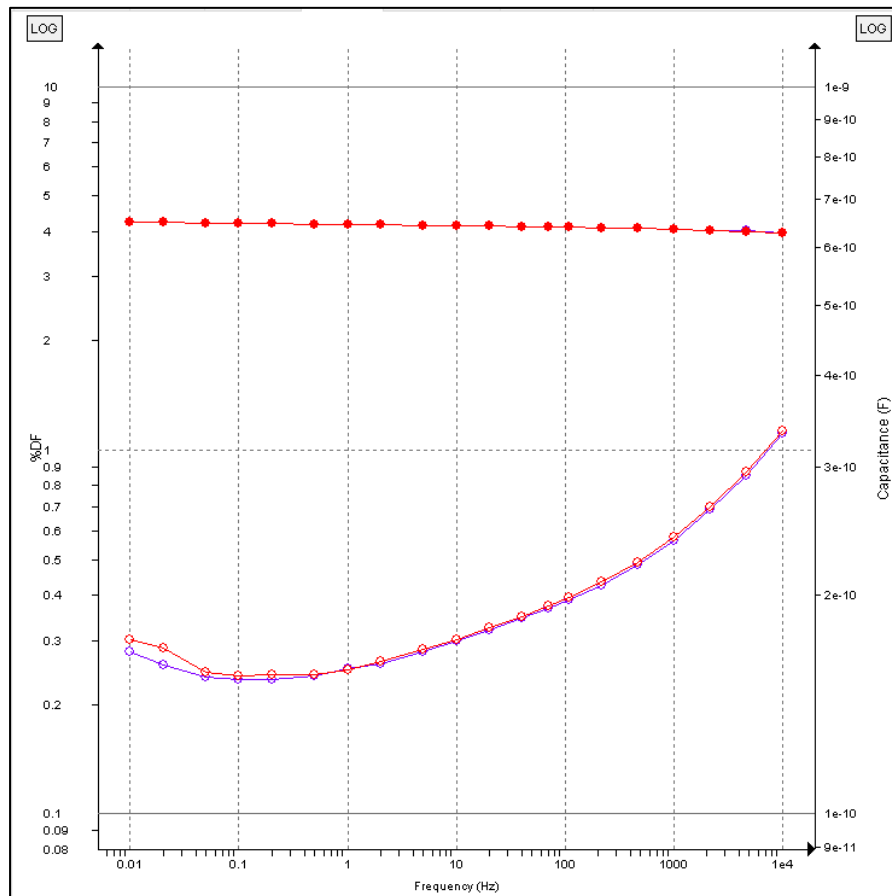


Figure 1: Capacitance (upper curve) and dissipation factor (lower curves) for a 245 kV RIP (Resin Impregnated Paper) bushing

From the curve, the following data can be extracted:

Frequency	Dissipation factor	Capacitance
50 Hz	% DF = 0.354	C = 641.8 pF
15 Hz	% DF = 0.310	C = 643.5 pF
1 Hz	% DF = 0.250	C = 646.2 pF

From the assessment criteria in the international guides, it can be determined that this bushing is moisture-free and in excellent condition, or “as new”.

%DF @ 50 Hz & 20°C	%DF @ 15 Hz & 20°C	%DF @ 1 Hz & 20°C
<b>0,353</b>	<b>0,310</b>	<b>0,250</b>
< 0.40 % As new	< 0.60 % As new	< 0.80 % As new
0.40 - 0.50 % Good	0.60 - 0.70 % Good	0.80 - 1.0 % Good
0.50 - 0.60 % Deteriorated	0.70 - 0.90 % Deteriorated	1.0 - 1.5 % Deteriorated
> 0.60 % Investigate	> 0.90 % Investigate	> 1.5 % Investigate

Figure 2: Assessment of RIP bushing and assessment criteria (screenshot from IDAX software)

Bushings are special in that, with relative ease, they can be tested at different temperatures, at least with less effort than it would take to manipulate the temperature of a power transformer. To show the effectiveness of the individual temperature correction (ITC) method used by IDAX, frequency sweeps at multiple temperatures are made for the same bushing as above. These temperatures are 20 °C (purple), 39.5 °C (grey), 45 °C (green), 54 °C (red), 69 °C (blue), and 85 °C (orange), respectively.

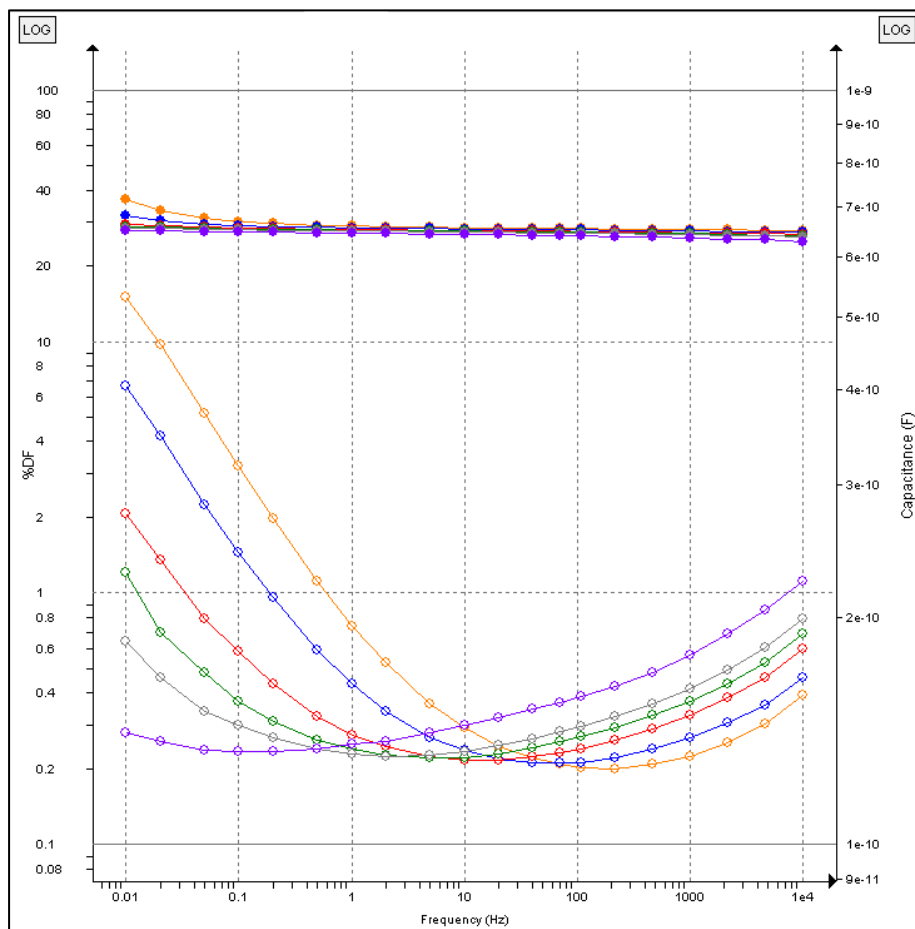


Figure 3: DRF sweeps 10 kHz to 10 MHz at multiple temperatures

As can be seen in Figure 3, the higher the temperature, the more to the right the shape of the dissipation factor curve is pushed.

The capacitance curve on the other hand, does not, as expected, change very much with increasing temperature. Upon closer inspection, the capacitance increases somewhat at lower frequencies and with increasing temperatures. This is, however, in line with the behaviour of many insulating materials.

In Figure 4, the individual frequency sweeps measured at 20, 39.5, 45, 54, 69, and 85 °C are transferred to the reference temperature of 20 °C using ITC and then plotted on top of each other.

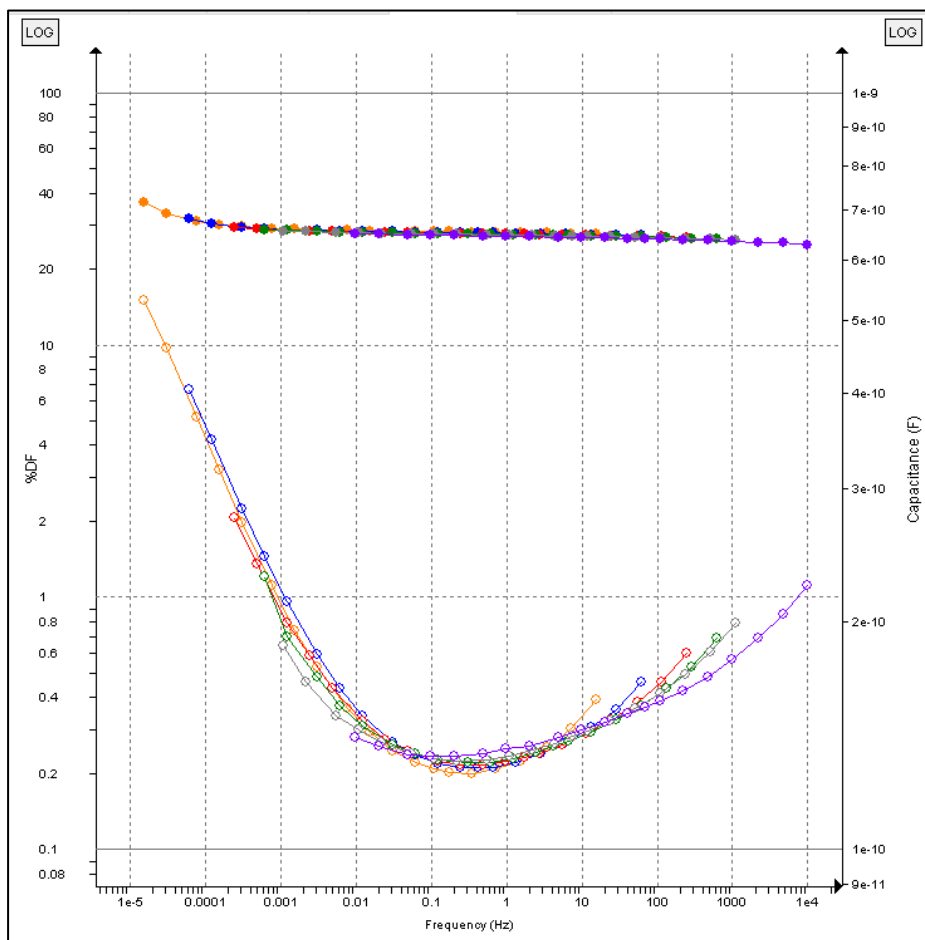


Figure 4: DFR sweeps at multiple temperatures translated to 20 °C using ITC

As can be seen in Figure 4, the different curves almost perfectly align, showing that DFR with ITC is an effective method for assessing bushing high temperature behaviour using data collected at a lower temperature.

There is a small deviation in the topmost frequencies of each curve (1 kHz to 10 kHz), but this is most likely due to a slight measurement error or influence from other factors than just the insulation of the bushing.

The capacitance readings also align well. If inspected closer, small discrepancies in alignment can be seen, something that possibly can be connected to slight changes in geometry with increasing temperature. ITC only takes the material properties into account.

### Modelling of a bushing with connection issues

In order to predict the DFR behaviour of a bushing with internal connection issues, a mathematical model needs to be created. In this model, we introduce capacitances (C) and resistances (R) between the innermost foil and the winding tube (a), and also between the outermost foil and the innermost foil (b) in a parallel and serial arrangement. Sometimes  $C_a$  is also referred to as  $C_0$ .

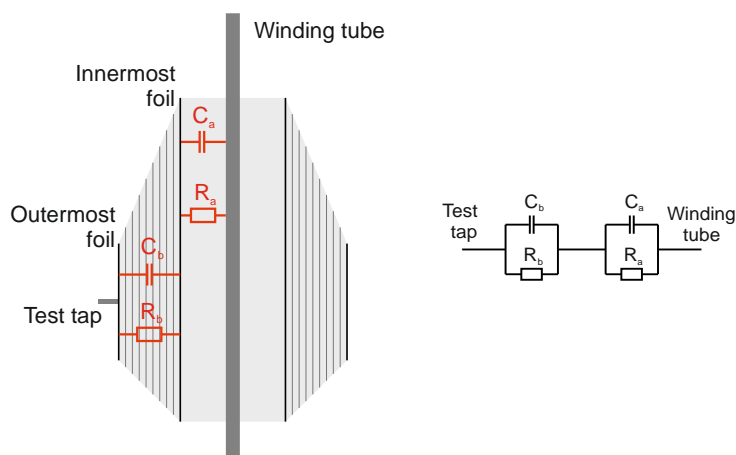


Figure 5: Electrical modelling of bushing with connection issues (dimensions exaggerated)

Starting from a model for two layered materials, the total admittance (Y) (inverted impedance) over the layers can be expressed as a function of the angular frequency ( $\omega$ ), the capacitance (Ck), and conductance (Gk) (inverted resistance =  $1/R_k$ ) of the respective layers, wherein k = "a" and "b".

$$Y = \frac{\omega^2(G_a C_b^2 + G_b C_a^2) + G_a G_b (G_a + G_b)}{(G_a + G_b)^2 + \omega^2(C_a + C_b)^2} + j\omega \frac{\omega^2(C_a + C_b)C_a C_b + C_a G_b^2 + C_b G_a^2}{(G_a + G_b)^2 + \omega^2(C_a + C_b)^2}$$

For the bushing, we assume that  $G_b = 0$ , meaning that there is infinite electrical resistance in the main body of the bushing. This simplifies the equation into:

$$Y = \frac{\omega^2 G_a C_b^2}{G_a^2 + \omega^2(C_a + C_b)^2} + j\omega \frac{\omega^2(C_a + C_b)C_a C_b + C_b C_a^2}{G_a^2 + \omega^2(C_a + C_b)^2}$$

Also, since we know that in a parallel circuit:

$$Y = \frac{1}{R_{parallel}} + j\omega C_{parallel}$$

or using IDAX terminology:

$$Y = j\omega(C' - jC'')$$

we can identify the real and complex parts of the admittance and calculate the tan delta value according to:

$$\tan \delta = \frac{C''}{C'}$$

To our model we also add a component taking the total equivalent resistance from test tap to winding tube into account, as well as a component to add to the normal tan delta response of the bushing. For simplicity, in the following examples, a fixed base value of 0.3 % over all frequencies is used.

### Modelling example 1: RIP bushing in good condition

In this example, a RIP bushing is modelled. The innermost foil of this bushing is intentionally shorted by the manufacturer to the winding tube to avoid electric stress between the innermost foil and the winding tube.

Designation	Value	Description
$C_a$	14 nF	Capacitance between innermost foil and winding tube, shorted and therefore very low capacitance
$C_b$	690 pF	Capacitance between outermost foil and innermost foil, $\approx C1$ value of bushing
$C_a$ and $C_b$	658 pF	Total capacitance from winding tube to test tap, calculated from $C_a$ and $C_b$ , if $R_a$ is infinite
$R_a$	0.3 m $\Omega$	Resistance shorting $C_a$ section
Base tan delta	0.3 %	Base losses of normal bushing, same value used for all frequencies

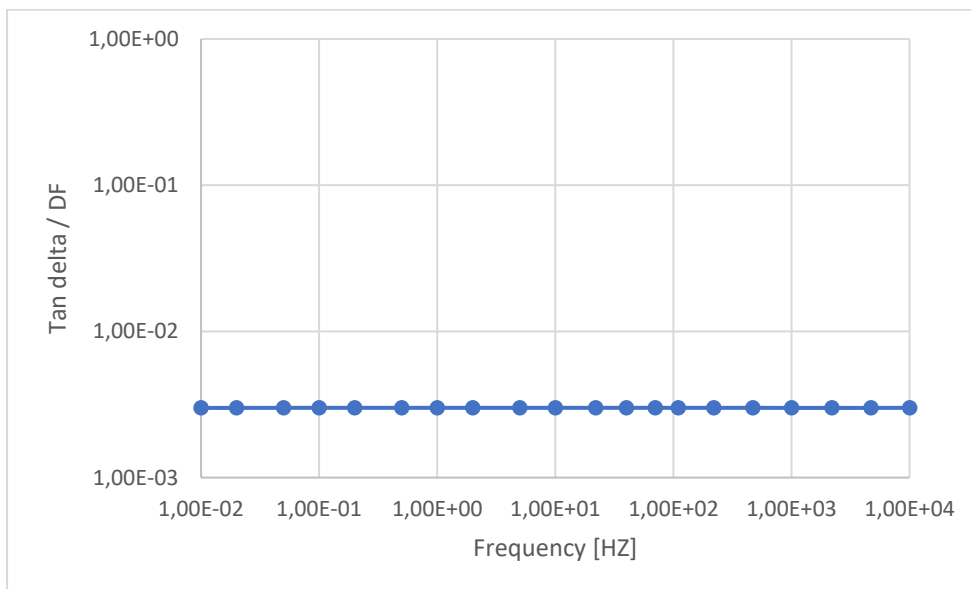


Figure 6: Graph showing the results for a bushing in good condition

As expected, the bushing exhibits a flat frequency response determined by the 'Base tan delta' of 0.3 %.

### Modelling example 2: RIP bushing with a poor “a” connection

In this example, a RIP bushing with a poor connection between the innermost foil and the winding tube is simulated.

Designation	Value	Description
$C_a$	14 nF	Capacitance between innermost foil and winding tube
$C_b$	690 pF	Capacitance between outermost foil and innermost foil, $\approx C1$ value of bushing.
$C_a$ and $C_b$	658 pF	Total capacitance from winding tube to test tap, calculated from $C_a$ and $C_b$ . if $R_a$ is infinite.
$R_a$	300 $\Omega$	Resistance shorting $C_a$ section
Base tan delta	0.3 %	Base losses of normal bushing, same value used for all frequencies

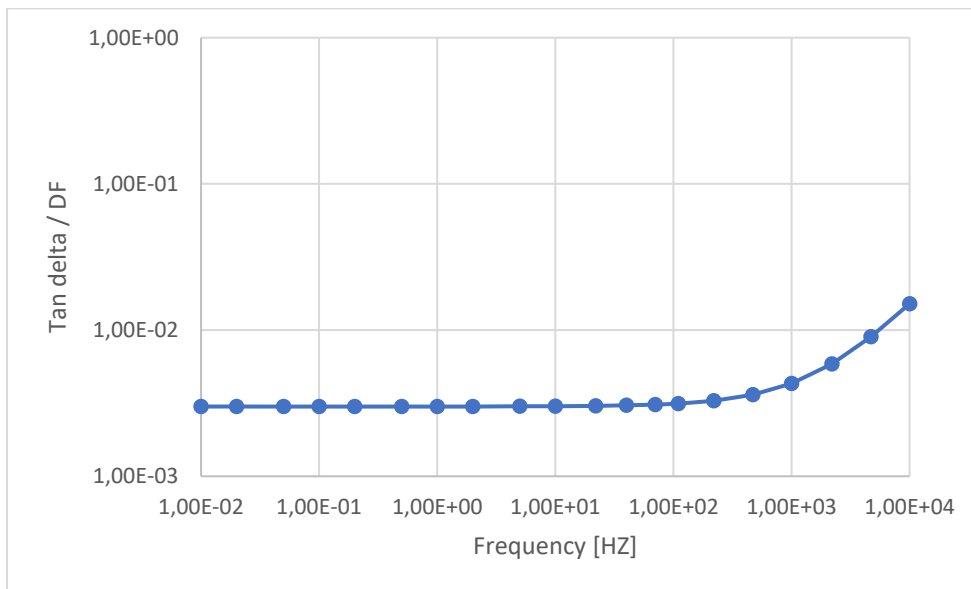


Figure 7: Graph showing a RIP bushing with a poor “a” connection

In this example, there is a clear increase in the dissipation factor values at higher frequencies. The higher the  $R_a$  value, the larger the increase at higher frequencies.



### Investigation of a suspected defective bushing

A RIP bushing with suspected connection issues between the winding tube and the innermost foil is tested using DFR at multiple temperatures, two of which are plotted in the graph below:

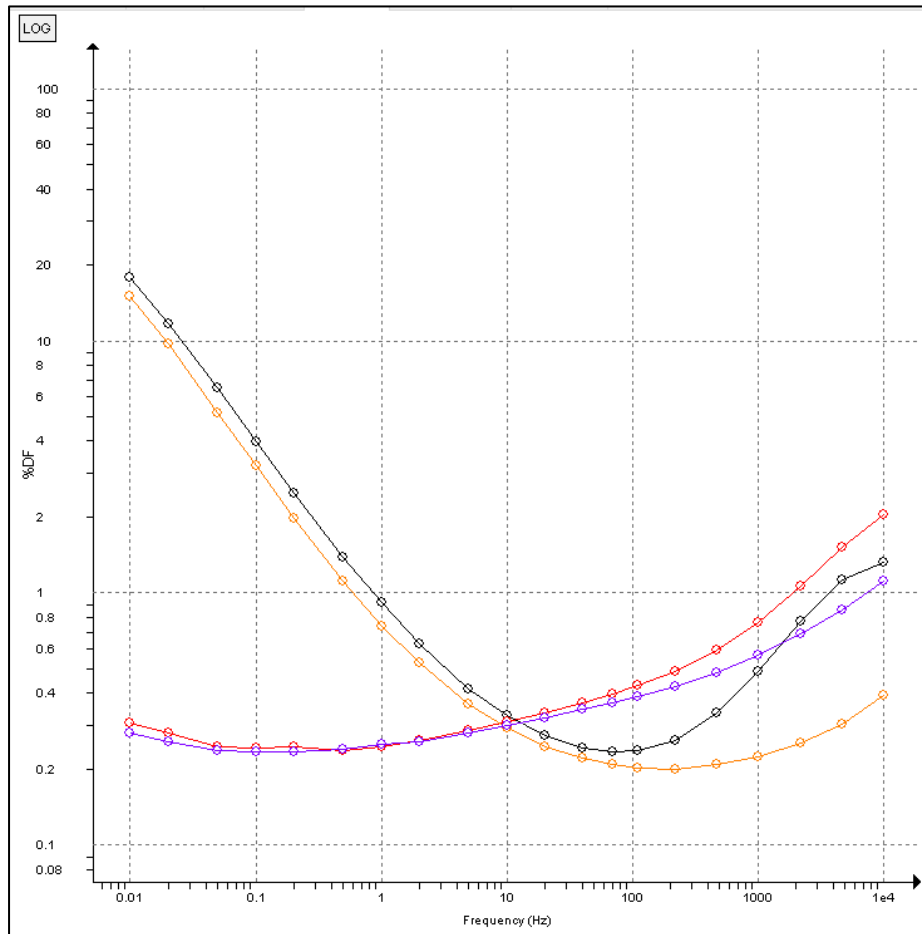


Figure 8: DFR response at 20 and 85 °C, respectively, of the reference bushing (purple and orange) and the bushing being investigated (red and black)

At lower frequencies, both bushings exhibit the same response but at higher frequencies, the bushing being investigated clearly exhibits a higher dissipation factor:

At 20 °C	Bushing	Investigated (red)	Reference (purple)	Difference
	50 Hz	% DF = 0.380	% DF = 0.353	+0.027
	1 kHz	% DF = 0.564	% DF = 0.763	+0.199
	10 kHz	% DF = 2.054	% DF = 1.109	+0.945
At 85 °C	Bushing	Investigated (black)	Reference (orange)	Difference
	50 Hz	% DF = 0.239	% DF = 0.216	+0.023
	1 kHz	% DF = 0.486	% DF = 0.224	+0.262
	10 kHz	% DF = 1.329	% DF = 0.391	+0.962

## Discussion

The RIP insulation temperature dependence is significant but well understood and can efficiently be modelled using the ITC algorithm. The bushing under investigation and the reference bushings have the same difference in 10 kHz tan delta at all temperatures investigated (8 °C to 85 °C), exemplified herein using 20 °C and 85 °C measurements. This suggests that it is possible to detect the contact problem using DFR up to 10 kHz in a wide range of temperatures.

Regarding the increase in dissipation factor at higher frequencies, this is consistent with modelling example 2, which implies that the bushing being investigated suffers from a poor connection between the winding tube and the innermost foil. As the increase in tan delta is the same for both temperatures, the mathematical model suggests that the resistance between the winding tube and the innermost foil does not change over the temperature range; a resistance  $R_a$  increasing with temperature would result in an even larger difference in tan delta between the investigated and reference bushings for the higher temperature.